Far-infrared and Raman analysis of phonons and phonon interface modes in GaN epilayers on GaAs and GaP substrates

G. Mirjalili,* T. J. Parker, S. Farjami Shayesteh,† M. M. Bülbül, and S. R. P. Smith
Department of Physics, University of Essex, Wivenhoe Park, Colchester CO4 3SQ, United Kingdom

T. S. Cheng and C. T. Foxon
Department of Physics, University of Nottingham, University Park, Nottingham NG7 2RD, United Kingdom
(Received 24 April 1997)

The vibrational properties of undoped α- and β-GaN epilayers on GaAs substrates have been investigated at 300 and 77 K by far-infrared Fourier transform spectroscopy using polarized oblique incidence reflectivity and Raman spectroscopy. These techniques have enabled us to determine the transverse- and longitudinal-optical phonon frequencies at the center of the Brillouin zone for propagation parallel and normal to the epilayers, as well as to investigate a number of interesting interface modes. Comparison of the phonon properties of a selection of GaN epilayers deposited by molecular-beam epitaxy on GaAs and GaP substrates indicates that their properties are strongly influenced by the substrate material and orientation. The presence of Berreman interface modes in the spectra is evidence of the presence of a boundary layer at the base of the GaN epilayer adjacent to the substrate. By modeling the boundary layer as a very thin ($\sim$15 nm in thickness) highly disordered region at the base of the GaN layer, all features in the measured spectra are satisfactorily assigned. [S0163-1829(98)01904-3]

INTRODUCTION

GaN has long been viewed as a promising system for semiconductor device applications in the blue and near-UV wavelength regions, but one of the major difficulties that has hindered GaN research is the lack of a suitable substrate material that is lattice matched and thermally compatible with GaN. Nevertheless, GaN has been grown on Si, GaAs, GaP, InP, NaCl, SiC, ZnO, Al_2O_3, $MgAl_2O_4$, TiO_2, and MgO substrates by a number of laboratories.[1] However, characterization of GaN epilayers on different substrates has not received sufficient attention.

In our previous work, far-infrared characterization of GaN epilayers in the cubic, wurtzite, and mixed phase on GaP substrates was reported.[2] In this paper we describe an investigation by polarized oblique incidence far-infrared reflection spectroscopy and Raman spectroscopy on samples consisting of thin epitaxial layers of GaN deposited by molecular-beam epitaxy (MBE) on GaAs substrates and compare these results with the earlier results.[2] The GaN layers are grown in the wurtzite (α-GaN) and cubic (β-GaN) phases. We have investigated the transverse- (TO) and longitudinal- (LO) optical phonon frequencies at the center of the Brillouin zone, as well as a number of interesting interface modes. These results are supported by Raman spectroscopy. A boundary layer at the GaN/substrate interface has been revealed in some of these systems. Comparison of the results obtained on the GaN/GaAs system with those of the GaN/GaP system shows in each case that the properties of the GaN epilayer are strongly influenced by the substrate material and orientation.

EXPERIMENTAL RESULTS AND ANALYSIS

Far-infrared (FIR) measurements were made using a modified NPL/Grubb Parsons modular cube interferometer. In this work six samples, each consisting of a thin epilayer of GaN on either a GaAs or a GaP substrate, have been investigated. The structure of the layers was either cubic or wurtzite and they were grown by MBE.[3] In the case of wurtzite-structure samples, the epilayers grow with the crystallographic *c* axis along the growth direction. All of the samples were undoped, and no free-carrier effects were observed for any sample in any of the measured spectra; further comments on this will be made in the relevant experimental sections. The basic parameters of these samples are tabulated in Table I, together with information on two samples, MG108 and MG85, described in an earlier publication,[2] which are included here for comparison.

The GaN FIR reststrahl region (450–800 cm^{-1}) is well separated in frequency from the GaAs (250–350 cm^{-1}) and GaP (350–450 cm^{-1}) reststrahlen regions. Stretched sheets of polyethylene terephthalate (Mylar) are commonly used as beam dividers in far-infrared spectrometers, the thickness being chosen to match the first transmission interference envelope to the required spectral range. However, it is not possible to choose a thickness that gives a good signal-to-noise

TABLE I. Basic parameters of the GaN epilayers investigated in this work.

Sample	Structure	Substrate	Thickness (μm)
MG107	Cubic	GaAs(001)	0.2
MG186	Cubic	GaAs(001)	0.6
MG217	Cubic	GaAs(001)	0.8
MG108	Cubic	GaP(001)	0.2
MG142	Wurtzite	GaAs(001)	0.2
MG159	Wurtzite	GaAs(001)	1.15
MG348	Wurtzite	GaAs(111)	1.15
MG85	Wurtzite	GaP(001)	0.6

ratio over the complete spectral range extending from 250–800 cm^{-1} using a single Mylar beam divider; furthermore, Mylar has a strong absorption band in the region 725–730 cm^{-1}, which adds to the difficulties of measurements in the GaN reststrahl region. Consequently, the experiments were carried out in each region using different beam dividers: we used a Mylar beam divider 6.25 μm in thickness for measurements in the GaAs reststrahl region, and for measurements in the GaN reststrahl region, a beam divider fabricated by depositing a thin film of Ge~0.50 μm in thickness on a parallel plate of KBr 0.5 cm in thickness was used.

FIR measurements were made in both *s*- and *p*-polarization. *s*-polarized measurements couple only to the component of the dielectric function parallel to the plane of the layers, whereas *p*-polarization measurements couple simultaneously to the components parallel and perpendicular to the plane of the layers, the relative contributions of the two components being determined by the angle of incidence. Thus, a combination of FIR measurements using both polarizations can be used to determine the dielectric parameters parallel and normal to the plane of the epilayers.

Calculated spectra were obtained using standard multilayer optics techniques,[4] the layers being vacuum for the medium of incidence, the GaN epilayer, and the substrate; in some samples it was also necessary to include in the model an additional thin (~15 nm in thickness) highly disordered layer at the base of the epilayer to account for the presence of an unexpected interface mode in the measured spectra.

We define Cartesian axes with $x=y$ normal to the growth direction, and z parallel to the growth direction. The dielectric function $\varepsilon_d(\omega)$ for each of the semiconductor layers was modeled using a classical dielectric function for a damped simple harmonic oscillator:

$$\varepsilon_{id}(\omega)=\varepsilon_{\infty,id}+\sum_j \frac{\rho_{id,j}\omega^2_{\mathrm{TO}id,j}}{\omega^2_{\mathrm{TO}id,j}-\omega^2-i\omega\gamma_{id,j}}, \qquad (1)$$

where $\omega_{\mathrm{TO}id,j}$, $\rho_{id,j}$, and $\gamma_{id,j}$ are, respectively, the transverse optical-phonon frequency, the phonon oscillator strength, and the phonon damping parameter of the jth oscillator in the ith layer in the dth direction ($d\equiv_\perp$ for the $x=y$ directions and $d\equiv_\parallel$ for the z direction). $\varepsilon_{\infty,d}$ is the limiting high-frequency value of the dielectric constant in the dth direction.

In the case of a sample with an ideal cubic structure, the epilayer would be isotropic and the dielectric function would be independent of direction, and we have an independent check on this: in the present work a single set of phonon parameters is sufficient to obtain a good fit to both the *s*- and the *p*-polarization spectra, indicating that there are no observable effects due to strain.

In the case of samples with the wurtzite structure, the overall symmetry is uniaxial with the uniaxis z oriented along the growth direction. Two sets of phonon parameters are therefore required to model the dielectric tensor: one to model $\varepsilon_{xx}(=\varepsilon_{yy})\equiv\varepsilon_\perp$ and another to model $\varepsilon_{zz}\equiv\varepsilon_\parallel$. For both sets we have used the published values for ε_∞ and ρ.[5] The mode frequencies, damping parameters, and layer thicknesses are determined from the experimental measurements described below. In the case of the cubic structure $\varepsilon_{xx}=\varepsilon_{yy}$ and ε_{zz} are equivalent, and both the mode frequency and all parameters except ε_∞ are determined experimentally.

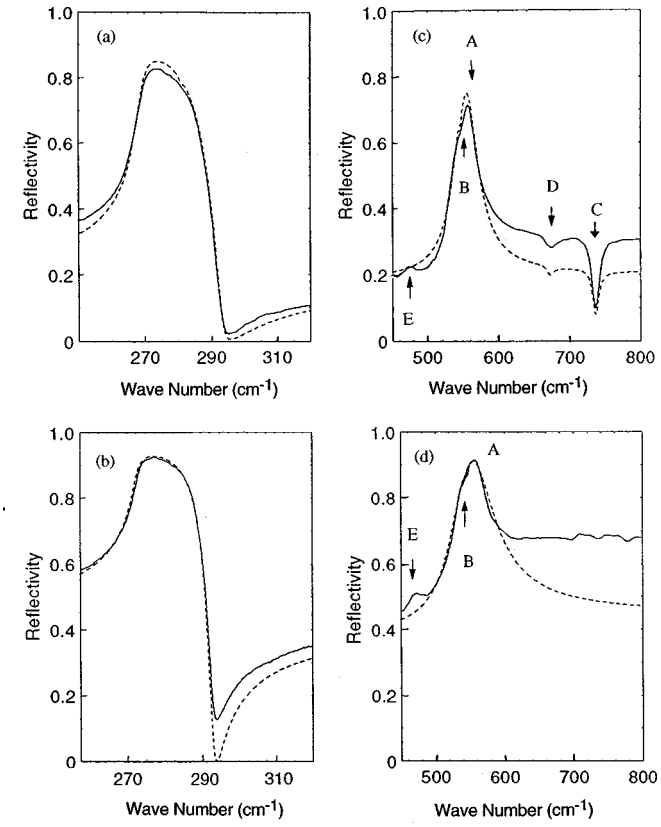

FIG. 1. Measured (solid lines) and calculated (dotted lines) far-infrared reflectivity spectra of a β-GaN epilayer on a GaAs substrate (sample MG107): (a) *p*-polarization spectrum and (b) *s*-polarization spectrum in the GaAs region; (c) *p*-polarization spectrum and (d) *s*-polarization spectrum in the GaN region. See text for discussion of marked features.

It is also possible to investigate so-called Brewster and Berreman interface modes[6,7] using the model. Dips in the *p*-polarization reflectivity, described as Brewster modes,[7] are observed when the numerator of the Fresnel reflection coefficient for an interface passes through zero due to impedance matching in the two media; a Berreman interface mode occurs in the vicinity of an LO phonon when the real part of ε crosses zero in one of the media if the real part of $\varepsilon<0$ in the second medium. Assignments of these modes can be made by calculating dispersion curves and the profiles of the electromagnetic fields throughout the structure. We show that the presence of an unexpected Berreman mode in the spectra of β-GaN samples can be used to obtain structural information on the samples, which is supported by results from electron microscopy.

The agreement between the experimental and theoretical curves is good in all cases. For simplicity we describe the behavior of the samples in each phase, i.e., cubic and wurtzite, respectively, in Secs. I and II, separately.

I. CUBIC PHASE (β-GAN)

Figures 1(a) and 1(b) show the *p*- and *s*-polarization FIR spectra of sample MG107 in the GaAs reststrahl region at 300 K. The epilayer is transparent in this region, so the spec-

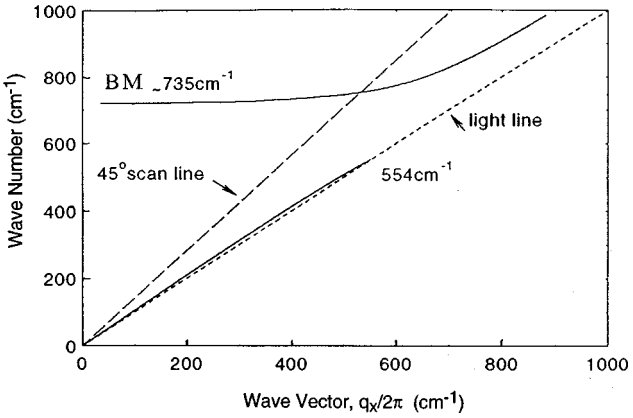

FIG. 2. Calculated dispersion curve for the Brewster mode (labeled BM) at the vacuum/β-GaN interface in sample MG107, indicating the presence of a Brewster mode at around 735 cm^{-1} at the intersection of the 45° scan line with the q_x curve. This point, which is associated with ω_{LO}, is observed as a dip in the p-polarization reflectivity spectrum, feature C in Fig. 1(c).

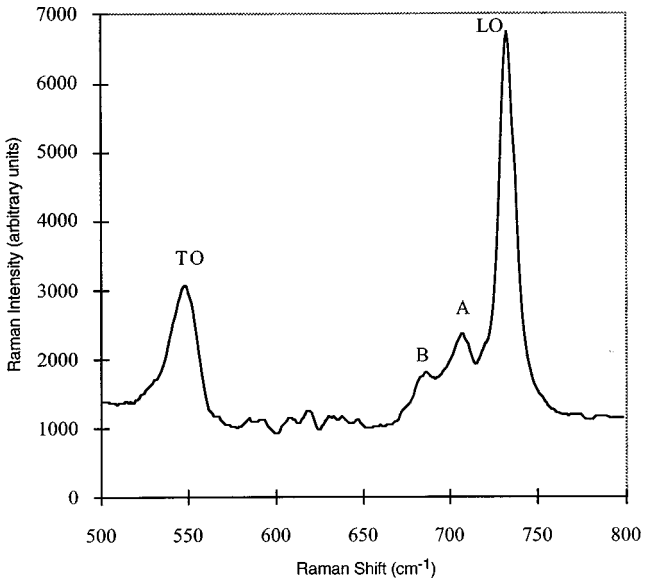

FIG. 3. Measured Raman spectrum of a β-GaN epilayer on a GaAs substrate (sample MG186) in backscattering $z(xy)\bar{z}$ configuration at room temperature, showing the LO and TO GaN zone-center phonons, a two-phonon combination band (A), and the boundary layer mode (B).

tra show only the reflection from the GaAs optical phonon band bounded by the TO frequency at 269.2 cm^{-1} and the LO frequency at 293.1 cm^{-1}.

Figures 1(c) and 1(d) show the p- and s-polarization spectra, respectively, for sample MG107 in the GaN reststrahl region at 300 K. Both spectra contain a pronounced peak A around 554 cm^{-1} near the β-GaN TO frequency, and a shoulder B near 547 cm^{-1}. The p-polarization spectrum has a pronounced dip C near 735 cm^{-1} and a weaker dip D near 684 cm^{-1}. Furthermore, there is a much weaker subsidiary peak E in both spectra near 475 cm^{-1}.

The main peak A near 554 cm^{-1} Figs. 1(c) and 1(d) corresponds to reflection from the GaN TO phonon mode and the large dip C at 735 cm^{-1} is associated with a Brewster mode[6] near the GaN LO phonon frequency at the vacuum/GaN interface. A calculated dispersion curve for this mode is shown in Fig. 2. The small peak E present in both the p- and s-polarization spectra is due to a two-phonon combination band in the GaAs substrate. Similar features have been observed before in bulk GaAs by many workers,[8–10] and no feature near 475 cm^{-1} is seen in any of our spectra of GaN epilayers on GaP substrates.[2] The shoulder B, near 547 cm^{-1}, and the dip D, at 684 cm^{-1}, however, are unexpected features, and their polarization properties imply that they correspond, respectively, to TO- and LO-like modes, as discussed below.

No free-carrier effects were observed in any of the spectra obtained with the samples used in this work. For instance, for this sample, MG107, no bulk free-carrier response was observed at frequencies below the GaAs reststrahl band. In the GaN LO phonon region, the effect of plasmon-phonon coupling is primarily to shift the Brewster mode near the LO frequency, with little effect on the background level. The frequency of the Brewster mode near to the GaN LO phonon (feature C) in Fig. 1(c) is close to the LO frequency of undoped GaN,[2] with no significant shift due to plasmon-phonon coupling. The difference in background levels of the measured and calculated spectra, most noticeably in Figs. 1(c) and 1(d) and in some later spectra, is therefore not associated with free-carrier effects, and most probably arises from an (unexplained) experimental artifact.

In Fig. 3 we show a typical Raman spectrum of β-GaN on a GaAs (001) substrate measured at 300 K using the 514.5 nm line of an Ar^+ laser operating at a power of $\sim$300 mW. The scattered light was analyzed using a Spex double monochromator and detected by standard photon-counting techniques. The spectrum was recorded with a spectral resolution of $\sim$2 cm^{-1} in the $z(xy)\bar{z}$ quasi-backscattering configuration (i.e., input and scattered beams propagating along z and $-z$, respectively, with input polarization along x and scattered polarization in the xy plane, where z is along the normal to the [001] surface, and x and y are the [100] and [010] directions). In this geometry, the selection rules permit scattering by LO modes with the wave vector parallel to [001].[11]

The spectrum shows two strong bands, namely, the TO and LO optical-phonon modes, at 552 and 738 cm^{-1}, respectively, in agreement with the infrared measurements and with previous Raman work on zinc-blende GaN.[12,13] The quality of the spectrum and the relative strengths of the LO and TO peaks vary at different places on the sample surface, indicating a variation in sample homogeneity and quality. In principle, TO scattering is forbidden for backscattering from a semi-infinite sample of perfect material but it becomes allowed when the scattering departs from strict backscattering; our experimental configuration departs from strict backscattering by a few degrees, but the presence of a forward-scattering component reflected from the substrate and deviations from 180° scattering caused by surface roughness are likely to be more significant in causing the observed TO scattering. We also observe two subsidiary modes, A at 710 ± 3 cm^{-1} and B at 684 ± 3 cm^{-1}, on the low-energy side of the LO band. The subsidiary peak A has been observed by others, e.g., Siegel *et al.*,[13,14] and is probably due to a two-phonon summation band originating from the combination of L-point LA and TO phonons. Zi *et al.*[15] have made first-principles calculations of the phonon-dispersion curves for

GaN, and quote the frequencies of these modes as 144 and 569 cm^{-1}, respectively (obtained by analysis of experimental data on the closely related hexagonal wurtzite structure). These values give a combination band at 713 cm^{-1}, in close correspondence with our observed frequency of 710 cm^{-1}. However, it is curious that this band is not observed in Raman scattering in hexagonal GaN,[14] where the 144- and 569 cm^{-1} modes are first-order allowed. The weak feature *B* at $\sim$684 cm^{-1} is attributed to the boundary layer mode observed in the FIR measurements, as no further two-phonon band is expected in this region. Although this layer is very thin, the GaN is actually transparent at the optical wavelength of the laser, 514.5 nm, and, if the boundary layer has a high optical absorption, scattering from this layer can be enhanced in backscattering. The Raman measurements therefore support the FIR assignment of the LO mode frequency of the boundary layer, which is discussed below.

We now turn to the interpretation of features *D* and *B* in Fig. 1(c). It can be seen that the dip *D* at 684 cm^{-1} is similar in shape to the shape of the Brewster interface mode *C* at 735 cm^{-1}. Experience with interface modes in other semiconductor structures[16] led us to consider that feature *D* might be associated with a Berreman mode, but this requires the existence of an additional interface in the structure.[7] If we postulate the existence of a very thin ($\sim$15 nm in thickness) boundary layer at the base of the GaN epilayer to create an additional interface within the GaN, the two conditions for the propagation of a Berreman mode along this interface are (i) that the LO phonon frequency in the boundary layer must occur at 684 cm^{-1} and (ii) that the real part of the dielectric response in the adjoining GaN layer must be negative at this frequency.[7] The second condition is automatically satisfied, since the GaN LO phonon frequency is greater than the proposed LO phonon frequency in the boundary layer. The thickness of the layer is determined from the model as it describes the magnitude of the dip at *D*. Detailed justification of this proposal is given below.

From the point of view of explaining the measured spectra using an additional layer, there are at least three possibilities for accounting for the presence of the two unexpected features (*B* and *D*).

(1) The boundary layer consists of an alloy of GaAs and GaN. The presence of such an alloy would shift the LO and TO phonon frequencies of bulk GaN and GaAs.[17] Although this might be an explanation of the additional features in the GaN region, there is no evidence of shifted LO or TO modes of bulk GaAs in the GaAs region of the spectrum, as can be seen from Figs. 1(a) and 1(b). Results from electron microscopy[18] on this sample also confirm that there is no evidence for the presence of a ternary compound of $GaAs_xN_{1-x}$. Thus, this possibility is untenable.

(2) The boundary layer is strained. However, phonon frequencies are expected to shift due to strain by only a few wave numbers,[19] so that the considerable shift of the LO frequency from 735 to 684 cm^{-1} cannot be explained by strain.

(3) The unexpected features arise from the presence of a very thin highly disordered boundary layer at the base of the GaN epilayer. Loss of periodicity in this heavily disordered layer would be expected to weaken the selection rules and cause all phonons to become infrared and Raman active.[20]

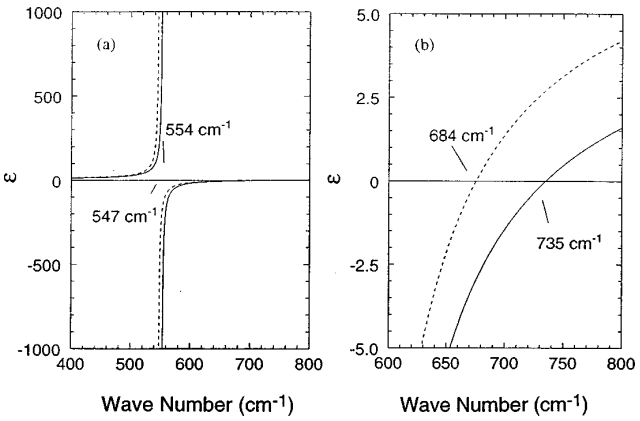

FIG. 4. The calculated dielectric functions ε, neglecting damping, for a β-GaN epilayer with a boundary layer on a GaAs substrate, e.g., sample MG107. The poles at 547 and 554 cm^{-1} correspond to the TO frequencies of the boundary layer and the β-GaN epilayer, respectively, and the zeros at 684 and 735 cm^{-1}, represent the LO frequency of the boundary layer and the β-GaN epilayer, respectively. Both scales expanded in (b) to illustrate the LO phonon region. Dashed line: boundary layer. Full line: β-GaN layer.

The zone-boundary frequencies in the III-V semiconductors are considerably lower than the zone-center frequencies,[21] so this would be expected to lower the frequency of the dielectric response in the boundary layer due to the dispersion of the optical-phonon branches of the dispersion curves across the Brillouin zone. We therefore assign feature *D*, which is only seen in *p* polarization, as a Berreman mode at the LO frequency of the boundary layer, and feature *B*, which is seen in both *s* and *p* polarization, as the TO frequency of the boundary layer. Calculated dielectric functions, neglecting damping, in the two layers are shown in Fig. 4 to illustrate this point; it can be seen from Fig. 4(b), in which both scales are expanded in the LO phonon region, that conditions (i) and (ii) stated above are indeed satisfied by this model. A calculated dispersion curve for the Berreman mode at 684 cm^{-1} at the interface between the GaN and the boundary layer is shown in Fig. 5.

Comparison of the lattice parameters of β-GaN and GaAs

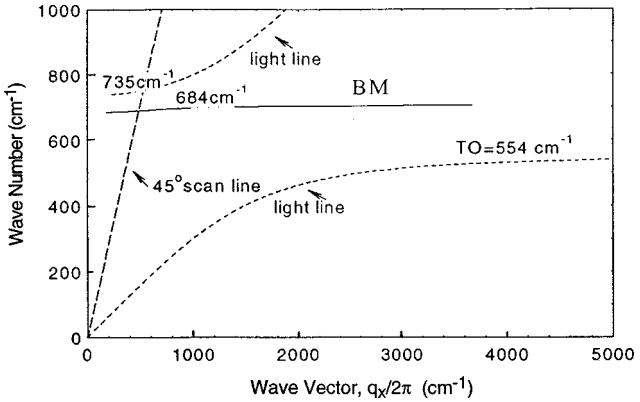

FIG. 5. Calculated dispersion curve for the surface polariton (i.e., the Berreman mode, labeled BM) at the interface of the good quality β-GaN epilayer and the boundary layer, e.g., sample MG107. A Berreman mode at 684 cm^{-1} is predicted at the point of intersection of the surface polariton dispersion curve and the 45° scan line, and appears as a dip in the *p*-polarization spectrum at *D* in Fig. 1(c).

TABLE II. The parameters used in modeling the spectra for cubic GaN epilayers on GaAs and GaP substrates. bl refers to the boundary layer.

	β-GaN/GaAs	β-GaN/GaP
ω_{TO} (cm^{-1})	554	553
ω_{LO} (cm^{-1})	735	733
ρ	4.1	4.05
γ (cm^{-1})	8	17
ω_{LO}(bl) (cm^{-1})	684	
ω_{TO}(bl) (cm^{-1})	547	
γ(bl) (cm^{-1})	11	$\sim$20
ε_∞	5.35	5.35

indicates that the lattice mismatch between the substrate and the GaN epilayer is about 22.3%. This very large mismatch creates many defects in the β-GaN epilayer, particularly in the region immediately above the substrate, creating the boundary layer. With increasing epilayer thickness, the GaN relaxes and reverts more or less to its bulk crystalline structure. Thus, in this model there are two regions within the GaN: a highly disordered boundary layer and an epilayer of much higher quality above it. The electron microscopy results[18] on this sample (MG107) show that the epilayer is a β-GaN single crystal with many extended defects on the {111} planes; the material immediately in contact with the substrate is heavily disordered, with a density of defects which decreases away from the GaN substrate interface.

In the case of β-GaN, the calculated phonon-dispersion curves[15,22] show that the LO phonon frequency drops from about 740 cm^{-1} at the zone center to about 640 cm^{-1} at the [001] zone boundary. The dispersion curve for the TO phonon, in contrast, is nearly flat, dropping only by about 15 cm^{-1} below 553 cm^{-1} in the [001] direction. This is consistent with the observed frequencies of the Berreman mode (feature D at 684 cm^{-1}) and the TO phonon mode (feature B at 547 cm^{-1}), which together define the effective LO and TO frequencies of the boundary layer.

If we pursue this further, we may model the boundary layer with a dielectric function

$$\varepsilon(\omega)=\varepsilon_\infty\left(1+\frac{\omega_{\mathrm{LO(bl)}}^2-\omega_{\mathrm{TO(bl)}}^2}{\omega_{\mathrm{TO(bl)}}^2-\omega^2-i\gamma_{(bl)}\omega}\right), \qquad (2)$$

where $\omega_{\mathrm{LO(bl)}}$, $\omega_{\mathrm{TO(bl)}}$, and $\gamma_{\mathrm{(bl)}}$ are, respectively, the LO and TO phonon frequencies and the phonon damping parameter in the boundary layer, and ε_∞ is the high-frequency dielectric constant of GaN. The damping parameter is nearly 40% greater than the damping parameter of the zone-center mode, which is consistent with line-broadening due to disorder. The parameters used for modeling in this case are listed in Table II.

We also find that with increasing thickness of the GaN epilayer the attenuation in the GaN layer eventually becomes too large and the coupling to the Berreman mode is lost. Thus, in a thicker sample, i.e., sample MG217 (0.8 μm thick), because $\varepsilon'<0$ in the GaN layer at 684 cm^{-1}, the radiation is strongly attenuated in the epilayer at this frequency, and the Berreman mode is not observed in this sample, as shown in Fig. 6(a). However, for sample MG186,

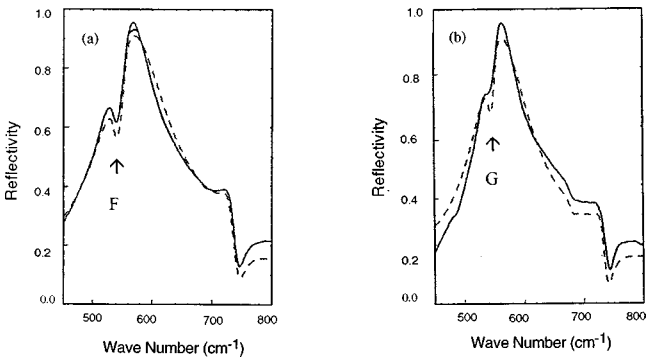

FIG. 6. Experimental (solid lines) and theoretical (dotted lines) p-polarization oblique incidence reflectivity spectra of β-GaN epilayers on GaAs substrates: (a) sample MG186 (thickness of epilayer=0.6 μm) and (b) sample MG217 (thickness of epilayer=0.8 μm). See text for a discussion of the marked features.

which has a GaN layer of intermediate thickness (0.6 μm), the Berreman mode is still just observed, as shown in Fig. 6(b). Features F and G are discussed later.

It is also found that the features at 547 cm^{-1} (B) and 684 cm^{-1} (D) measured at 300 K shift slightly after the sample is cooled to 77 K and rewarmed again, as shown in Fig. 7(a), indicating that the boundary layer is not stable. In contrast, the main features at 554 cm^{-1} (A) and 735 cm^{-1} (C), which are GaN mode frequencies, do not shift. This implies mechanical accommodation to temperature changes in the boundary layer which does not influence the good quality GaN epilayer above. Figure 7(b) shows that the GaN phonon frequencies, features A and C, increase slightly, as expected, on cooling to 77 K.

For the β-GaN/GaP system, i.e., sample MG108, the main features occur at 553 and 733 cm^{-1} corresponding to the β-GaN TO and LO phonon frequencies, respectively.[2] The p-polarization spectra of samples MG107 and MG108 are compared in Fig. 8. The phonon parameters of β-GaN/GaP are compared with those of β-GaN/GaAs in Table II, and it can be seen that the damping parameter for the β-GaN/GaP system is much larger than for the β-GaN/GaAs system, and the LO and TO frequencies are slightly different.

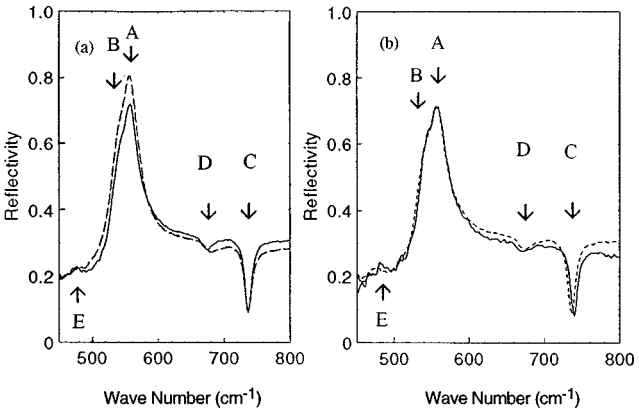

FIG. 7. (a) Comparison of the p-polarization reflection spectra of a β-GaN epilayer on a GaAs substrate (sample MG 107) measured at room temperature before (dotted line) and after (solid line) cooling down to 77 K and rewarming. (b) Comparison of the p-polarization spectra of the same sample at 77 K (solid curve) and at 300 K (dotted curve). See text for a discussion of the marked features.

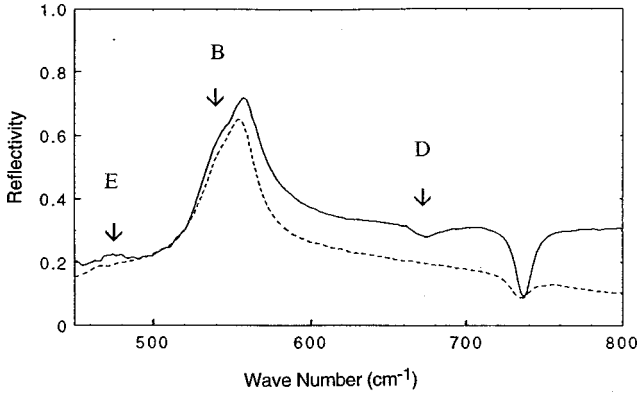

FIG. 8. Comparison of the p-polarization spectra of a β-GaN epilayer on a GaAs substrate (sample MG107, solid line) and a β-GaN epilayer on a GaP substrate (sample MG108, dashed line) at room temperature. The features marked by B and D, respectively, correspond to boundary layer phonon frequencies, and that marked by E corresponds to a two-phonon combination band in the GaAs substrate of sample MG107, which is absent in β-GaN/GaP. The linewidths of the peak and dip in β-GaN/GaAs are sharper than those in β-GaN/GaP, and occur $1-2\ \mathrm{cm}^{-1}$ higher in frequency.

The lattice mismatch between GaN and GaP is about 18.6% and results from electron microscopy indicate that similar defects occur at the boundary between the substrate and the GaN epilayer[23] as in β-GaN/GaAs, but no Berreman mode associated with a boundary layer is seen in this sample. Table II shows that in the GaN/GaAs system the damping parameter for the boundary layer found from the Berreman mode is nearly 40% greater than the phonon damping parameter in the good quality GaN epilayer. If we include a boundary layer in the model for sample MG108, with a phonon damping parameter of about $20\ \mathrm{cm}^{-1}$ for the Berreman mode, i.e., about 25% greater than for the main features, no Berreman mode is seen in the calculated spectrum. It therefore appears that the reason for the absence of the Berreman mode in the β-GaN/GaP system is just the larger phonon damping parameter.

In addition, dips in the spectra in s and p polarization are observed below the TO frequency at around $535\ \mathrm{cm}^{-1}$ for samples MG186 and MG217, i.e., those with the thicker epilayers (see Fig. 6, features F and G). These features are due to interference between the radiation reflected off the top surface of the GaN and that reflected off the GaN/GaAs interface. The frequency at which interference occurs is dependent on the layer thickness and the phase change on reflection at the GaN/GaAs interface.[2] Sample MG107 has too thin an epilayer for the dip to be resolved. We have used this dip as a measure of layer thickness. The presence of an interference dip in the spectra in this case has masked the TO frequency of the extra feature at $547\ \mathrm{cm}^{-1}$ and the weak feature at $475\ \mathrm{cm}^{-1}$ belongs to a two-phonon combination band. These features are not distinguishable in thicker samples.

II. WURTZITE STRUCTURE (α-GaN)

For the wurtzite structure, experiments at 300 and 77 K in both s and p polarization have been carried out on samples MG159, MG142 and MG348. The basic parameters for these samples are listed in Table I. We consider these samples as

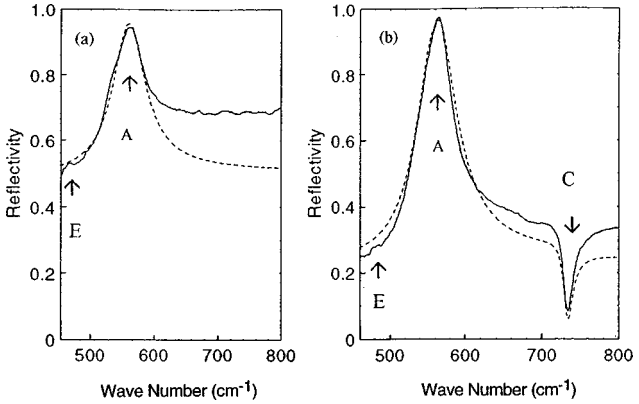

FIG. 9. Experimental (solid curves) and theoretical (dotted curves) spectra of an α-GaN epilayer on a GaAs substrate (a) in s- and (b) in p-polarization oblique incidence reflectivity, sample MG142. See text for a discussion of the marked features.

α-GaN/GaAs. The far-infrared properties of α-GaN/GaP (Ref. 2) will be compared with this system.

In this case, the GaN dielectric function has uniaxial symmetry. The s- and p-polarization spectra of samples MG142 and MG159, shown in Figs. 9 and 10 respectively, have the same appearance as for the cubic structure. However, the high-reflectivity feature at A in both s and p polarization occurs around a pole in ε_{xx} at the TO frequency and the dip at C in p polarization occurs at a zero in ε_{zz}, an LO frequency. Since there are no prominent features at the zero in ε_{xx} and the pole in ε_{zz} the oscillator strengths cannot be accurately measured for these samples. For this reason we have based our modeling on the measured values of ω_{TO} for $E\perp z$ and ω_{LO} for $E\|z$, together with published values for the oscillator strengths.[5] $\omega_{\mathrm{LO}\perp}$ and $\omega_{\mathrm{TO}\|}$ have been calculated by using the Lyddane-Sachs-Teller relation.[24] A weak subsidiary peak at E corresponding to a phonon combination band in the GaAs substrate is also revealed in the thinner epilayer (sample MG142), Fig. 9.

In Table III, the parameters used for the α-GaN/GaAs system at 300 K are compared with those obtained for the α-GaN/GaP system.[2] We used $\varepsilon_{\infty\perp}=\varepsilon_{\infty\|}=5.35$ for the wurtzite phase.[25]

Comparison between the spectra in the GaN region of samples MG348 and MG159, Fig. 11, shows that the peaks

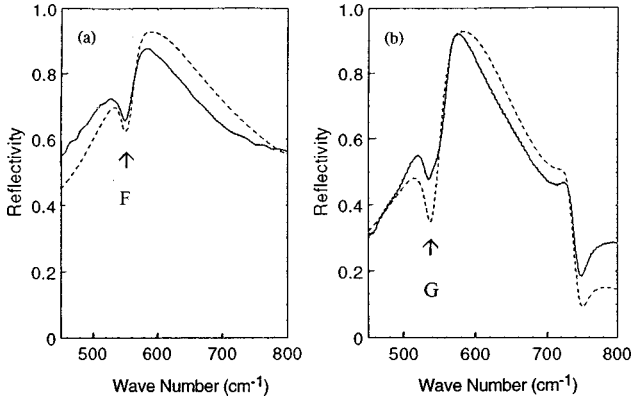

FIG. 10. Experimental (solid curves) and theoretical (dotted curves) oblique incidence reflectivity spectra of an α-GaN epilayer on a GaAs substrate (a) in s and (b) in p polarization, sample MG159. Features F and G as in Fig. 6.

TABLE III. The parameters used in modeling the spectra for wurtzite GaN epilayers on GaAs (001) and (111) substrates, and GaP (111) substrates.

Sample	$\omega_{TO\perp}$ E_1(TO) (cm^{-1})	$\omega_{LO\perp}$ E_1(TO) (cm^{-1})	$\gamma_\perp$ (cm^{-1})	$\omega_{TO\parallel}$ A_1(TO) (cm^{-1})	$\omega_{LO\parallel}$ A_1(TO) (cm^{-1})	$\gamma_\parallel$ (cm^{-1})	γ (substrate region) (cm^{-1})
α-GaN/GaAs(001)	560[a]	744[b]	10[a]	530[b]	740[a]	11[a]	30[a]
α-GaN/GaAs(111)	560[a]	744[b]	6[a]	530[b]	740[a]	7[a]	17[a]
α-GaN/GaP(001)	560[a]	744[b]	38[a]	529[b]	739[a]	65[a]	77[a]

[a]Derived from far infrared data.
[b]Derived using the oscillator strength, Ref. 5.

and dips in the two spectra occur at the same points; this implies that, firstly, the thickness, and secondly, the TO and LO frequencies, of GaN epilayers grown on GaAs (001) and (111) substrates are very similar. However, the sharpness of the features in the spectra of sample MG348, compared with those of sample MG159, indicate that the damping parameter for GaN grown on a (111) GaAs substrate, i.e., sample MG348, is significantly less than that of sample MG159 grown on a (001) GaAs substrate. Furthermore, in both the *s*- and *p*-polarization spectra of sample MG348, a shoulder, marked by an arrow, occurs around 544 cm^{-1}; this feature is a second-order interference feature that is revealed in modeling when using small damping parameters. The parameters using in modeling sample MG348 are listed in Table III.

In the wurtzite structure there is also a large mismatch between the α-GaN epilayer and the GaAs substrate. According to results obtained on wurtzite-structure GaN epilayers on GaP substrates by electron microscopy there is a defect region on top of the substrate but with a different nature compared with that in cubic epilayers:[23] the defects are, respectively, planar and columnar in cubic and wurtzite phase GaN epilayers. No extra features have been seen in wurtzite-structure epilayers, either with a GaAs or a GaP substrate. This may suggest that the presence of extra features is dependent on the nature of the defects in the boundary layer, i.e., the defect regions in the boundary layers in cubic and wurtzite-structure epilayers have different dielectric properties.

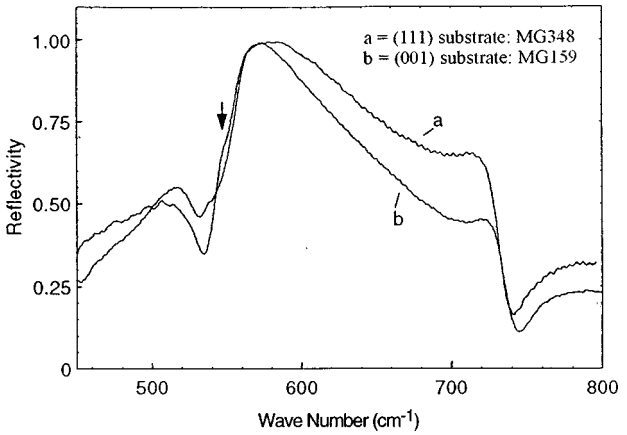

FIG. 11. Comparison of the *p*-polarization reflectivity spectra of the α-GaN/GaAs system grown on substrates cut in different directions; *a* and *b* refer to sample MG348 and sample MG159, respectively.

As mentioned in Sec. I the feature around 535 cm^{-1} for a thicker epilayer, Fig. 11, arises from interference. The position of this feature is sensitive to the GaN layer thickness. We have, therefore, used it as a measure of layer thickness as before. There is an increase of about $1-3\ cm^{-1}$ for the optical-phonon mode frequencies of GaN at 77 K.

CONCLUSIONS

In this work we have measured the *s*- and *p*-polarized far-infrared reflectivity spectra at 45° angle of incidence and the Raman spectra of α-GaN and β-GaN epilayers on GaAs. The key spectroscopic results for β-GaN epilayers on GaAs substrates are observed using both techniques. The previous[2] and the present studies are complementary: we have now determined all infrared-active phonon frequencies and several dielectric parameters in the different phases of GaN epilayers deposited by MBE on GaAs and GaP substrates. Furthermore, it has been established that the presence of extra features in the spectra that are associated with a Berreman mode is dependent on the presence of a defect GaN region on top of the substrate that is created during growth. However, the defects in α- and β-GaN epilayers have different dielectric properties. There is a small discrepancy between the phonon frequencies of GaN deposited on GaAs and GaP substrates that may be related to the percentage of mismatch between the substrate and the epilayer. The damping parameters in α-GaN/(111) GaAs are much smaller than in α-GaN/(001) GaAs. Overall, the damping parameters for GaN epilayers grown on a GaP substrate are extremely large, implying poorer quality samples.

In doped GaN epilayers the Brewster and Berreman modes discussed here couple strongly to plasmons propagating normal to the plane of the epilayers. In a planned subsequent paper,[26] we show how analysis of these coupled modes can be used to investigate the effective masses of electrons and holes in *n*- and *p*-type GaN epilayers parallel and normal to the planes of the epilayers.

ACKNOWLEDGMENTS

We wish to thank EPSRC for financial support. G.M. wishes to acknowledge financial support by the Islamic Republic of Iran and the University of Yazd and S.F.S. wishes to acknowledge financial support from the University of Gilan. M.M.B. wishes to thank Gazi University in Turkey for research leave and financial support.

*Present address: Department of Physics, University of Yazd, P.O. Box 89195-714, Yazd, Iran.
†Present address: Faculty of Science, Gilan University, P.O. Box 1914, Rasht, Iran.

[1] S. Strite and H. Morkoc, J. Vac. Sci. Technol. B **10**, 4 (1991).
[2] G. Mirjalili, T. Dumelow, T. J. Parker, S. Farjami Shayesteh, T. S. Cheng, C. T. Foxon, L. C. Jenkins, and D. E. Lacklinson, Infrared Phys. Technol. **37**, 389 (1996).
[3] C. T. Foxon, T. S. Cheng, S. V. Novikov, D. E. Lacklinson, L. C. Jenkins, D. Johnston, J. W. Orton, S. E. Hooper, N. Baba-Ali, T. L. Tansley, and V. V. Tretyakov, J. Cryst. Growth **150**, 892 (1995).
[4] T. Dumelow, T. J. Parker, S. R. P. Smith, and D. R. Tilley, Surf. Sci. Rep. **17**, 151 (1993).
[5] A. S. Barker, and M. Ilegems, Phys. Rev. B **7**, 743 (1973).
[6] D. W. Berreman, Phys. Rev. **130**, 2193 (1963).
[7] T. Dumelow and D. R. Tilley, J. Opt. Soc. Am. A **10**, 633 (1993).
[8] T. Sekine, K. Uchinokura, and Matsuura, J. Phys. Chem. Solids **38**, 1091 (1977).
[9] C. Patel, Ph.D. thesis, University of London, 1982.
[10] Y. D. Harker, C. Y. She, and D. F. Edward, J. Appl. Phys. **15**, 272 (1962).
[11] W. Hayes and R. Loudon, *Scattering of Light by Crystals* (Wiley, New York, 1978).
[12] S. Miyoshi, J. Cryst. Growth **124**, 439 (1992).
[13] H. Siegel, L. Eckey, A. Hoffmann, C. Thomsen, B. K. Meyer, D. Schikora, M. Hankenl, and K. Lischka, Solid State Commun. **96**, 943 (1995).
[14] H. Siegel, G. Kaczmarcztk, L. Filippids, A. P. Litvinchuk, A. Hoffmann, and C. Thomsen, Phys. Rev. B **55**, 7000 (1997).
[15] J. Zi, X. Wan, G. Wei, K. Zhang, and X. Xie, J. Phys.: Condens. Matter **8**, 6323 (1996).
[16] A. A. Hamilton, T. Dumelow, T. J. Parker, and S. R. P. Smith, J. Phys.: Condens. Matter **8**, 8027 (1996).
[17] O. K. Kim and W. G. Spitzer, J. Appl. Phys. **130**, 4362 (1979).
[18] P. D. Brown and C. J. Humphreys (private communication).
[19] F. Cerdeira, C. J. Buchenauer, F. H. Pollak, and M. Cardona, Phys. Rev. B **5**, 580 (1972).
[20] D. D. Klug and E. Walley, J. Chem. Phys. **56**, 553 (1972).
[21] *Crystal and Solid State Physics, Landolt-Bornstein, New Series, T Group III*, Vol. 22, pt. a (Springer-Verlag, Berlin, 1987).
[22] Jian Zi, W. Guanghong, Z. Kaiming, and X. Xide, J. Phys.: Condens. Matter **8**, 6329 (1996).
[23] Y. Xin, P. D. Brown, R. E. Dunin-Brokowski, and C. J. Humphreys, J. Cryst. Growth **171**, 321 (1997).
[24] R. H. Lyddane, R. G. Sachs, and E. Teller, Phys. Rev. **59**, 673 (1941).
[25] E. Ejder, Phys. Status Solidi A **6**, 445 (1971).
[26] G. Mirjalili, R. A. Levett, T. J. Parker, T. S. Cheng, and C. T. Foxon (unpublished).